Published in final edited form as:
Free Radic Biol Med. 2008 October 15; 45(8): 1094–1102. doi:10.1016/j.freeradbiomed.2008.07.007.

Catalase ameliorates polychlorinated biphenyl-induced cytotoxicity in non-malignant human breast epithelial cells

Venkatasubbaiah A. Venkatesha[1], **Sujatha Venkataraman**[1], **Ehab H. Sarsour**[1], **Amanda L. Kalen**[1], **Garry R. Buettner**[1], **Larry W. Robertson**[2], **Hans-Joachim Lehmler**[2], and **Prabhat C. Goswami**[1,*]

1*Free Radical and Radiation Biology Program, Department of Radiation Oncology, The University of Iowa, Iowa City, Iowa*

2*Occupational & Environmental Health, The University of Iowa, Iowa City, Iowa*

Abstract

Polychlorinated biphenyls (PCBs) are environmental chemical contaminants believed to adversely affect cellular processes. We investigated the hypothesis that PCB-induced changes in the levels of cellular reactive oxygen species (ROS) induce DNA damage resulting in cytotoxicity. Exponentially growing cultures of human non-malignant breast epithelial cells (MCF10A) were incubated with PCBs for 3 days and assayed for cell number, ROS levels, DNA damage, and cytotoxicity. Exposure to 2,2',4,4',5,5'-hexachlorobiphenyl (PCB153) or 2-(4-chlorophenyl)benzo-1,4-quinone (4-Cl-BQ), a metabolite of 4-chlorobiphenyl (PCB3) significantly decreased cell number, MTS reduction, and increased the percentage of cells with sub G_1 DNA content. Results from electron paramagnetic resonance (EPR) spectroscopy showed a 4-fold increase in the steady-state levels of ROS, which was suppressed in cells pre-treated with catalase. EPR measurements in cells treated with 4-Cl-BQ detected the presence of a semiquinone radical, suggesting that the increased levels of ROS could be due to the redox-cycling of 4-Cl-BQ. A dose-dependent increase in micronuclei frequency was observed in PCB-treated cells, consistent with an increase in histone 2AX-phosphorylation. Treatment of cells with catalase blunted the PCB-induced increase in micronuclei frequency and H2AX phosphorylation that was consistent with an increase in cell survival. Our results demonstrate a PCB-induced increase in cellular levels of ROS causing DNA damage, resulting in cell killing.

Keywords

polychlorinated biphenyls; oxidative stress; DNA damage; MCF10A; antioxidants; catalase; free radical

INTRODUCTION

Polychlorinated biphenyls (PCBs) are environmental pollutants that are known to elicit a broad spectrum of adverse effects both in animals and humans. PCBs were widely used as coolants and lubricants in transformers and as a dielectric in capacitors [1]. The production of PCBs

*Address for correspondence to: Prabhat C. Goswami, PhD, B180 Medical Laboratories, The Free Radical & Radiation Biology Program, Department of Radiation Oncology, The University of Iowa, Iowa City, IA 52242-1181, Fax: 319-335-8039, E-mail: prabhat-goswami@uiowa.edu.

was discontinued in the USA in 1977. Their continued use in closed system, high thermal stability and persistent bioaccumulation raised concerns about their safety [1,2]. The commercial production of PCBs gave rise to complex mixtures, including many individual isomers and congeners. The biological effects of individual PCBs are determined by the number and position of chlorines in the biphenyl rings, which also determines their chemical and physical properties.

Epidemiological studies indicate increased mortality of capacitor and electric utility workers from various cancers [3–7]. Besides, recent evidences suggest that exposure to PCBs might be casually linked to an increased incidence of breast and prostate cancer [8–11]. Previous studies reported the presence of different PCBs in human breast milk [12,13]. 2,2',4,4',5,5'-hexachlorobiphenyl (PCB153) is a non-metabolizable PCB commonly found in breast milk suggesting that chronic exposure to PCB153 could adversely affect cellular processes. Consistent with this hypothesis, PCB153 exposure has been shown to cause cell death in rat cerebellar granule cells [14]. 2-(4-chlorophenyl)benzo-1,4-quinone (4-Cl-BQ) is a metabolite of 4-chlorobiphenyl (PCB3) [15]. 4-Cl-BQ is believed to undergo redox-cycling resulting in the generation of reactive oxygen species (ROS). Several PCBs are believed to mediate their cellular effects by altering cell proliferation and cell death. PCB104, PCB3, and PCB5 have shown to increase cell proliferation in endothelial and MCF-7 cells by different mechanisms [16,17], while PCB153 and PCB77 were shown to be cytotoxic in rat cerebellar granule cells [14]. The mechanisms regulating PCB-induced perturbations in cellular proliferation and cell death are not completely understood. We hypothesize that PCB-induced changes in the steady state level of ROS regulate cell proliferation and cell death.

The steady state level of ROS is a balance between production of ROS and their removal by antioxidants. ROS (*e.g.* superoxide, hydrogen peroxide) are produced intracellularly by two metabolic sources: the mitochondrial electron transport chain and enzymatic reactions. ROS are well known to damage cellular macromolecules including DNA. Increased peroxide levels have been observed with exposure to PCB77 or PCB126 in marine invertebrates [18]. Exposures to PCBs and dioxin-like PCBs are reported to result in oxidative stress in wild life animals [19]. Human breast cancer (T47D and MDA-MB-231) and promyelocytic (HL-60) cells exposed to PCB153, PCB126, or PCB-hydroquinones caused DNA damage [20,21]. PCB153 has been shown to form DNA-adducts [22], and because DNA adducts are known to cause DNA damage and mutations, it is hypothesized that PCB-induced DNA damage could result in toxicity.

DNA damage can be assessed by measuring the frequency of micronuclei formation and phosphorylation of histone 2AX. Micronuclei arise from acentric chromosome fragments or a whole chromosome that lags behind during cell division. Several studies have reported that ionizing radiation-induced DNA damage correlates with an increase in the frequency of micronuclei [23–25]. H2AX, a minor variant of histone 2A, is phosphorylated via ataxia telangiectasia mutant (ATM) in response to radiation [26]. Because H2AX-phosphorylation (Ser139) is one of the earliest events in radiation-induced DNA damage, γH2AX (phosphorylated H2AX) is considered a predictive marker for DNA damage and cellular responses to oxidative stress [27].

In this study, we investigated the hypothesis that PCB-induced changes in ROS levels result in DNA damage and cytotoxicity in human nonmalignant breast epithelial cells. MCF10A non-malignant human breast epithelial cells exposed to 4-Cl-BQ and PCB153 showed increased ROS levels, which were associated with increases in micronuclei frequency and γH2AX protein levels indicative of DNA damage. The PCB-induced increase in DNA damage enhanced cytotoxicity. These effects were suppressed in cells pre-treated with catalase supporting the hypothesis that ROS regulate biological responses to PCB exposures.

MATERIALS & METHODS

Cell culture and reagents

MCF10A, non-malignant human mammary epithelial cells, was purchased from American Tissue Culture Collection (ATCC). MCF10A cells are spontaneously immortalized diploid cells that possess the characteristics of normal breast epithelium. Cells were cultured in mammary epithelial cell growth medium (MEGM) supplemented with growth factors and antibiotics (Cell Applications Inc.). Monolayer cultures were grown at 37°C in a humidified incubator with 5% CO_2 and 95% air. Cytochalasin-B, Acridine Orange, Hoechst 33352 (bisbenzamide), catalase, and polyethylene glycol-conjugated (PEG) catalase were from Sigma Chemical Co. 3-(4, 5-Dimethylthiazol-2-yl)-5-(3-carboxymethoxyphenyl)-2-(4-sulfophenyl)-2H-tetrazolium (MTS) was from Promega. 5, 5-Dimethyl-1-pyrroline N-oxide (DMPO) was from Dojindo Laboratories.

2-(4-Chlorophenyl)benzo-1, 4-quinone (4-Cl-BQ) and 2,2',4,4',5,5'-hexachlorobiphenyl (PCB153) were synthesized and characterized as described previously [28,29]. The purity of the PCBs was determined by gas chromatography and found to be >98%. PCB stock solutions were prepared using dimethyl sulfoxide; the final concentration of DMSO in culture medium was kept below 0.5%. Control cultures were adjusted to the same concentrations of DMSO as the PCB-treated cells.

Asynchronously growing exponential cultures of MCF10A were treated with 1–5 μM PCBs for 3 days. PCB dose selection was based on a recent study where it was reported that the blood levels of PCBs in individuals living in Anniston, Alabama varied from 0 – 6.5 μM [30].

Cell growth assays

Cell growth was measured following trypsinization by counting cells in a Z1 Coulter Counter (Beckman Coulter) and the MTS assay. For the MTS assay, monolayer cultures in 96-well dishes were rinsed with sterile PBS followed by the addition of 100 μL media containing MTS (0.765 nM) and phenazine methosulfate (25 μM) [31]. The plate was incubated in CO_2 incubator at 37°C for 2 hours; the amount of formazan bioreduction was measured at 485 nm in a multi-plate reader.

Cell survival assays

Monolayer cultures were trypsinized and re-plated at limited dilutions. Cells were cultured for 14 days and stained with 1% crystal violet in 1% methanol. Surviving colonies, each containing 50 or more cells, were scored. Plating efficiency was used to calculate surviving fraction, and results were normalized relative to untreated control.

In a separate series of experiments, flow cytometry was used to measure cell viability following our previously published protocol [32,33]. Monolayer cultures were trypsinized, and cell suspensions incubated with 1 μg propidium iodide (PI) mL^{-1} PBS. PI-fluorescence was measured by flow cytometry (BD FACScan) with Argon Ion Laser, 488 nm excitation and 585 nm band pass filter. Data were collected from 10,000 cells in list mode; the percentages of PI-positive (representative of non-viable cells) and PI-negative (representative of viable cells) were calculated using the WinMDI software.

PI staining of ethanol-fixed cells followed by flow cytometry assay of DNA content was used to measure percentage of cells with sub G_1 DNA content following our previously published protocol [32,33].

DNA damage assays

Micronucleus assay and phosphorylation levels of histone 2AX were used to measure DNA damage. The micronucleus assay used in this study was a modified protocol [23] of the original method of Fenech and Morley [34]. Briefly, control and PCB-treated monolayer cultures were incubated with fresh medium containing cytochalasin-B (4 μg mL^{-1}) and continued in PCB-free culture medium for 2 days. Cells were harvested by trypsinization; cell pellets fixed in Carnoy-fixative solution (methanol: acetic acid, 3:1). Fixed cells were spread onto pre-cleaned coded slides and stained with 0.0125% acridine orange in Sorensen's buffer (pH 6.8). Stained cells were visualized under a fluorescent microscope with excitation wavelength set at 453 nm and a 450–490 nm band pass filter (Olympus BX-51). A minimum of four hundred bi-nucleated cells with well-preserved cytoplasm were scored for each treatment. The frequency of micronucleated bi-nucleate cells (MNBNC) was calculated following the scoring criteria guidelines [35].

Phosphorylated H2AX protein levels were detected in control and PCB-treated cells grown in four-chamber slides (Lab-Tek). Monolayer cultures were fixed in 4% para-formaldehyde for 15 min at room temperature, washed and blocked in blocking solution containing Dulbecco's phosphate-buffered saline (DPBS) and goat serum (5%). Cells were stained with Texas-red phalloidin (1:1000) for 1 hour at room temperature. The monolayers were then washed with DPBS containing 0.2% Triton-X, re-blocked, incubated with 1:500 anti-phosphorylated histone H2AX (Ser139) antibody (Upstate Biotech) for 1 hour at 37°C followed by incubation with goat anti-mouse IgG conjugated with Alexa Fluor 488 secondary antibody (1:800). Cells were stained with HOECHST (1:500) for 20 min, and slides were cover-slipped under aqueous mounting agent (Lerner Laboratories). Fluorescent signals from 3 different channels were visualized using appropriate filters in an inverted fluorescent microscope (Leica DMIRE2).

Immunoblotting assay

Monolayer cells in exponential growth were harvested with trypsinization and protein extracts were prepared by sonication. Equal amounts of protein were separated on 12.5% sodium dodecylsulfate-polyacrylamide gel electrophoresis and electro-transferred by semidry blotting onto a nitrocellulose membrane. Membranes were incubated with antibodies to phosphorylated histone 2AX (Upstate Biotech) and actin. Immunoreactive bands were visualized by an enhanced chemiluminescence kit (GE Healthcare). Results were quantitated using AlphaImager 2000 software (Alpha Innotech) and calculated relative to actin levels in individual samples. Fold-change was calculated relative to untreated control.

Electron Paramagnetic Resonance (EPR) spectroscopy

EPR spectroscopy with DMPO as the spin trap was used to measure the production of free radicals in control and PCB-treated cells. Exponentially growing asynchronous cultures of MCF10A (control and cells treated with PCB for 3 days) were rinsed with PBS and covered with 500 μL of chelated (iminodiacetic acid, sodium form, Sigma) [36] PBS containing DMPO (100 mM). Cells were then incubated at 37°C for 15 min, scraped, and transferred to a flat cell for EPR measurement. Cells were incubated with CuZnSOD (1000 U mL^{-1}) or catalase (300 U mL^{-1}) prior to the EPR measurement to determine if changes in EPR-signals were due to PCB-induced alterations in superoxide versus hydrogen peroxide. EPR peak heights were determined and normalized to 1×10^6 cells [32,37]. Sample volumes for all EPR experiments were 500 μL. EPR measurements were made using a Bruker EMX 300 spectrometer (TM cavity with flat cell) with a magnetic field modulation frequency of 100 kHz and nominal microwave power of 40 mW. Spectra were collected with modulation amplitude of 1.0 G, scan rate 80 G/81 s, receiver gain $10^4 – 10^6$, and an average of 20 scans. Spectral analyses were done by simulation of experimental spectra using the NIEHS simulation program [37].

To determine if PCB-associated semiquinone radicals are formed in cells, we did direct EPR measurements of cell suspensions. Cells were treated with 4-Cl-BQ (30 μM) for 12 hours. Then the cell monolayer was washed, scraped-harvested and suspended in chelated PBS at pH 7.4 or PBS pH = 10 (by addition of NaOH). These samples were then analyzed for semiquinone radical formation.

Measurement of extracellular hydrogen peroxide

The measurement of extracellular hydrogen peroxide was performed following a previously published protocol [38]. This method is based on hydrogen peroxide reacting with horseradish peroxidase (HRP) to form compound I, followed by a subsequent reaction where compound I reacts with *p*-hydroxyphenyl acetic acid (*p*HPA) forming a stable fluorescent dimer, $[pHPA]_2$. MCF10A cells were treated with 3 μM of PCB for 3 days; cells were washed with phenol red–free Hanks' buffered saline solution (HBSS) and incubated with 1.0 mL HBSS supplemented with glucose (6.5 mM), HEPES (1 mM), sodium bicarbonate (6 mM), *p*HPA (1.6 mM), and HRP (95 μg mL^{-1}) at 37°C for 1 hour. The amount of H_2O_2 released into the buffer was measured spectrofluorometrically at 20 min intervals for 60 min using excitation and emission wavelengths of 323 and 400 nm, respectively. The fluorescent intensity of each sample was corrected for any changes in pH. The absorbance of hydrogen peroxide at 240 nm was used to prepare standards.

Statistics

Statistical significance was determined by one-way ANOVA and Student t-tests. Results are presented as mean ± standard error of mean. Homogeneity of variance was assumed with 95% confidence interval level. Results from at least $n \geq 3$ with $P < 0.05$ are considered significant.

RESULTS

PCB exposures perturb cellular proliferation

To determine if exposure to PCBs perturb proliferation in nonmalignant human breast epithelial cells, exponentially growing asynchronous cultures of MCF10A were exposed to 0 – 5 μM PCBs for 3 days and analyzed for cell growth and viability. After a 3-day treatment with 3 μM 4-Cl-BQ the number of cells decreased approximately 40%; treatment with PCB 153 (3 or 5 μM) decreased the cell number by approximately 70% (Figure 1A). The decrease in cell numbers in PCB153 treated cells correlated with the decrease in MTS reduction (Figure 1B).

PCB-induced perturbation in cellular proliferation was also evident from results presented in Figure 1C&D. Monolayer cultures of control and PCB-treated cells from replicate dishes were stained with PI and fluorescence measured by flow cytometry. The percentage of PI-positive (non-viable) cells after treatment with 5 μM PCB153 was approximately 30% compared to untreated cells. Cells treated with 3 μM 4-Cl-BQ showed approximately 10% non-viable cells (Figure 1C). Toxicity induced by PCB153 was also evident from an increase in the percentage of cells with sub G_1 DNA content. Treatment with 3 μM PCB153 resulted in approximately 10% of the cells with sub G_1 DNA content, while 5 μM had approximately 25% (Figure 1D).

PCB exposures perturb cellular steady-state levels of ROS

To determine if PCB-induced perturbations in cellular proliferation are associated with changes in the steady-state levels of cellular ROS, EPR spin-trapping was performed. Cells (untreated or treated with PCB, 3 days) were incubated with DMPO and EPR spectra recorded, Figure 2A and B. The EPR spectra show a typical 1:2:2:1 DMPO-OH quartet (closed circles, Figure 2A-i) accompanied by additional spectral lines. Computer simulation indicated that these additional spectral lines are consistent with the presence of a carbon-centered radical adduct

of DMPO (Figure 2A-iii), and a small contribution from a simple nitroxide radical (Figure 2A-iv). The hyperfine splitting constants of the carbon-centered radical adduct of DMPO are consistent with the methyl adduct [39]. This is most likely due to the reaction of hydroxyl radical with DMSO (solvent used to dissolve PCBs).

The EPR spectrum of the 1:2:2:1 DMPO-OH quartet (Figure 2A-ii) can originate from: (1) the covalent addition of superoxide; or (2) hydroxyl radical generated *via* the Fenton reaction. To distinguish whether the DMPO-OH quartet signal could be due directly to superoxide or to H_2O_2, PCB-treated MCF10A cells were incubated with either CuZnSOD or catalase 30 min prior to the addition of DMPO. Addition of SOD did not significantly alter EPR peak heights in 4-Cl-BQ-treated cells suggesting that the DMPO-OH signal is not directly due to superoxide radical (data not shown). However, treatment with catalase suppressed 4-Cl-BQ-induced increase in EPR peak heights (Figure 2B-iii and 2C) suggesting that hydroxyl radical generated from the reaction of metals with hydrogen peroxide could be the specific ROS reacting with DMPO. Results (Figure 2C) show that 3 μM of 4-Cl-BQ or PCB153 increased the steady-state levels of cellular ROS approximately 2- to 3-fold, compared to DMSO-treated controls ($P < 0.05$). Catalase pre-treatment suppressed the 4-Cl-BQ-induced increase in EPR peak heights, suggesting that exposure to PCBs increases cellular hydrogen peroxide levels.

To determine if cells exposed to PCBs have increased rates of production of H_2O_2, we examined the level of extracellular H_2O_2, Figure 3A. PCB-treated cells were incubated with HBSS buffer containing HRP and *p*HPA, and the amount of H_2O_2 released was measured spectrofluorometrically. Both 4-Cl-BQ and PCB153 treatments showed a significant increase in extracellular levels of H_2O_2 compared to controls. This increase was suppressed in cells pre-treated with catalase (Figure 3A).

There is considerable evidence that semiquinone radicals can be a primary source for formation of H_2O_2 from the hydroquinone/quinone redox system [40–42]. To determine whether semiquinone radical is formed in cells as a result of exposure to oxygenated PCBs, direct EPR measurements of semiquinone radical were performed. When cells were suspended in pH 7.4 buffer (1.5×10^6 cells mL^{-1}) and examined by EPR for semiquinone radical, cells exposed to 4-Cl-BQ showed a weak singlet at g = 2.005, Figure 3B-ii; whereas cells not exposed to 4-Cl-BQ had no such signal (Figure 3B-i). Because higher pH increases the rate of autoxidation of hydroquinones (and quinones) and stabilizes semiquinone radicals [40], we repeated the measurement after adjusting the pH of the cell suspension to 10. Indeed, the intensity of the EPR spectrum of this species increased considerably, Figure 3B-iv; again, no such signal was observed in cells not exposed to 4-Cl-BQ (Figure 3B-iii). These spectra are consistent with an immobilized semiquinone radical as observed by Guo *et al.* [43]. These observations indicate that semiquinone radicals are indeed formed in cells; this species could be the source of the apparent higher flux of H_2O_2 observed.

PCB-induced an increase in levels of cellular ROS resulting in DNA damage

The micronucleus assay was performed to determine if PCB-induced increases in the steady-state levels in cellular ROS would lead to DNA damage. Exponentially growing asynchronous cultures were treated with different concentrations of PCBs for 3 days. The medium was removed at the end of the PCB treatments and fresh medium containing cytochalasin B was added. Cells were cultured for additional 2 days and harvested for the micronucleus assay. Cells irradiated with 3 Gy were used as a positive control for the assay. Representative microscopic pictures of micronuclei and nucleoplasmic bridge are shown in Figure 4A. Quantitation of data is presented in Figure 4B&C and Table I and Table II. The percentage of cells bearing one micronucleus per cell was minimal (~3%) in DMSO-treated control cells (Figure 4B and C, Table I and Table II). However, PCB exposures resulted in a dose-dependent increase in percentage of cells with one, two or multiple micronuclei (Table I). The frequency

of MNBNC increased 4-fold in 0.5 μM and 7-fold in 3 μM 4-Cl-BQ treated cells. PCB153 treated cells also showed a dose-dependent increase in MNBNC frequency. The frequency of MNBNC in 5 μM PCB153-treated cells was similar to 3 μM 4-Cl-BQ-treated cells. Overall, the frequency of single micronuclei per cell was more common compared to two and multiple micronuclei per cell (Table I and II). 4-Cl-BQ and PCB153 treated cells showed nucleoplasmic bridge.

To further determine if the PCB-induced increase in cellular ROS levels caused DNA damage, cells were treated with PEG-catalase prior to and during the PCB treatments. Control and PCB-treated cells in the presence or absence of catalase were harvested for the micronuclei assay (Figure 4C and Table II). The frequency of micronuclei in cells exposed to 1 μM 4-Cl-BQ was 16%, which decreased to 10% in cells treated with PEG-catalase. The frequency of micronuclei in cells exposed to 3 μM PCB153 was approximately 12%, which decreased to approximately 8% in cells pre-treated with PEG-catalase (Figure 4C and Table II).

The PCB-induced increase in the steady-state levels of cellular ROS and subsequent DNA damage was further evident from the results presented in Figure 5. Exponentially growing cultures were exposed to PCBs (3 μM) for 3 days and processed for the microscopy assay for phosphorylated H2AX (γH2AX). Monolayer cultures were immunostained for γH2AX (Figure 5A, middle panel) and counterstained for DNA and cytoskeleton (Figure 5A, left panel). The overlay of the pictures of the nucleus, cytoskeleton, and γH2AX are shown in Figure 5A (right panel). The frequency of γH2AX foci was low in DMSO-treated control cells and high in PCB treated cells. Treatment with 4-Cl-BQ resulted in numerous γH2AX foci (diffused and punctuate staining) compared to PCB153 (fewer foci). It is interesting to note that treatment with PCB153 caused morphological changes compared to control and 4-Cl-BQ treated cells.

Consistent with the results obtained from the microscopy assay, PCB treatment elevated γH2AX levels (Figure 5B, compare lane 1 with lanes 2 and 3). γH2AX protein levels in cells exposed to 1 μM 4-Cl-BQ were comparable to 3 μM PCB153, suggesting that 4-Cl-BQ could be more cytotoxic. Treatment of cells with PEG-catalase prior to and during the PCB-exposures significantly suppressed the PCB-induced increase in γH2AX protein levels (Figure 5B, lanes 4 and 5). These results are consistent with the results presented in Figure 4 and Table I and Table II, supporting the hypothesis that the PCB-induced increase in cellular ROS levels caused DNA damage.

PCB-induced increase in cellular ROS levels is cytotoxic

To determine if the PCB-induced increase in cellular ROS levels and subsequent DNA damage resulted in cytotoxicity, cell numbers and survival were measured. Exponentially growing asynchronous cultures of MCF10A were treated with 1 μM 4-Cl-BQ or 3 μM PCB153 for 3 days. At the end of the 3-day treatment monolayer cultures were washed and continued in culture in fresh medium without PCBs. Monolayer cultures were trypsinized at the end of 7 days, and cell proliferation measured by counting cell numbers. A 75% decrease in cell number was observed in cells exposed to 4-Cl-BQ, while exposure to PCB153 exhibited a decrease of approximately 25% in cell growth (Figure 6A). This PCB-induced decrease in cell number was partially abrogated in cells treated with PEG-catalase prior to or during the exposure to PCBs.

Cells from replicate dishes were trypsinized and re-plated at limiting dilution for clonogenic cell survival assay. Cells were fixed and stained at the end of the 14-day incubation, and surviving colonies with at least 50 cells per colony were counted. Normalized survival fraction (NSF) was calculated relative to control. NSF decreased approximately 50% in cells exposed to 1 μM 4-Cl-BQ, compared to 30% decrease in cells treated with 3 μM of PCB153 (Figure 6B). PEG-catalase suppressed PCB153-induced cytotoxicity while the same pre-treatment did not alter 4-Cl-BQ-induced cytotoxicity.

DISCUSSION

PCBs are environmental pollutants known to cause numerous biological effects. Although mechanisms regulating these adverse biological effects are not completely understood, our results show exposure to PCBs increased levels of H_2O_2 in MCF10A non-malignant human breast epithelial cells. The PCB-induced perturbations in the levels of cellular ROS resulted in DNA damage and cytotoxicity. The selection of PCB153 in this study was based on its high stability and higher levels in human milk of PCB-exposed individuals [12]. While the mechanisms regulating PCB153-induced toxicity is not completely understood, there is some evidence that PCB153 is an agonist to the constitutive androstane receptor (CAR) [44]. 4-Cl-BQ has a quinone "like" structure and was therefore thought to undergo redox-cycling leading to increased ROS levels.

The concentrations of PCBs used in this study were within the range found in people exposed to PCBs. In general, serum levels of PCBs in Americans average about 10 ppb (≈ 30 nM); whereas occupationally exposed individuals may have PCB blood levels in the hundreds of ppb [45]. PCB blood levels in individuals living in Anniston, Alabama vary widely (0.003 – 6.5 μM) [reviewed in 29]. PCB levels in adipose tissue are much higher than those in blood, with levels in low ppm range [46]. Once ingested and absorbed, PCBs may remain in the body for extended time periods. Since physiologically relevant PCB levels can be in the micromolar range we chose to test the effect of 0.5 – 5 μM PCBs in nonmalignant human breast epithelial cells, MCF10A.

Our results show that exposure to PCBs perturb cellular proliferation in MCF10A cells. PCB-induced perturbations in cellular proliferation were associated with changes in cellular ROS levels, suggesting that ROS-signaling could regulate cellular responses to PCB exposures. Recent evidence, including our research, suggests ROS-signaling could influence multiple cellular processes regulating cell proliferation, differentiation, and cell death [33,47–53]. These observations are consistent with: (*a*) our earlier observations of cell cycle phase-specific changes in cellular ROS levels; (*b*) the necessity of a pro-oxidant event prior to S-entry; (*c*) the protection of cellular proliferative capacity by MnSOD; and (*d*) differing intracellular redox environments during the cell cycle of normal *versus* cancer cells [32,48,49,52,53]. Results from these reports suggest that fluctuations in the intracellular cellular redox environment could function to regulate numerous cellular processes.

The cellular redox environment is influenced by the flux of ROS and their removal by antioxidants. ROS (superoxide, hydrogen peroxide) are primarily produced intracellularly by two metabolic sources: the mitochondrial electron transport chain and oxidase enzymes. Numerous external agents (*e.g.* radiation and oxidative stress causing chemicals) are also known to alter cellular steady-state levels of ROS. Although ROS levels are tightly regulated by antioxidants, an imbalance will result in increased oxidative stress that could be detrimental to cells. Our results show that while exposure to 4-Cl-BQ and PCB153 increased extracellular hydrogen peroxide levels, treatment with catalase blunted this effect. This is in line with the mechanistic observations of Song *et al.* demonstrating that oxygenated PCBs, such as 4-Cl-BQ, can lead to the production of H_2O_2 [40]. Our results indicate H_2O_2 as the specific ROS that could cause damage to cellular macromolecules (Figure 3A).

A key observation of this study is that catalase blunted the 4-Cl-BQ-induced increase in DMPO-OH levels while the same treatment did not significantly affect the PCB153-induced increase in DMPO-OH levels (Figure 2C). These results suggest that different PCB congeners could have different mechanisms for inducing oxidative stress. 4-Cl-BQ could undergo redox-cycling resulting in increased production of $O_2^{\bullet-}$ and H_2O_2. An increased flux of $O_2^{\bullet-}$ would result in an increased flux of H_2O_2. Hydrogen peroxide in the presence of redox active metals

would undergo Fenton chemistry, yielding highly damaging hydroxyl radicals. Consistent with this hypothesis EPR measurements in 4-Cl-BQ-treated cells detected a semiquinone radical (Figure 3B). This radical can be the source of H_2O_2.

PCB153 is known to be a CAR-agonist that induces CYP-2B [44]. However, it is currently unknown if a direct or indirect interaction of PCB153 with receptors could result in ROS production. The biological effects of PCB153 could also be due to its ability to form DNA adducts [22]. Furthermore, the differences in the biological effects of PCBs could also depend on their structure, aromaticity, halogenation and presence of other substitutions on the biphenyl ring.

Our results showed that the PCB-induced increase in cellular ROS levels was associated with a dose-dependent increase in micronuclei formation (Figure 4). Although exposure to both PCBs exhibited increased frequency of micronuclei, individual variations did occur. For example, 4-Cl-BQ-induced micronuclei formation occurred at a much lower dose than PCB153-treated cells. In general, both PCBs generated a higher percentage of MNBNC with one micronucleus compared to two and multiple micronuclei (Table I and Table II). The frequency of multiple micronucleus and nucleoplasmic bridge was higher in PCB153 and 4-Cl-BQ treated cells compared to control. PCB-induced DNA damage was also evident from microscopic and immunoblotting results of γH2AX protein levels (Figure 5). Because elevated γH2AX protein levels are indicative of DNA double strand breaks, our results indicate that exposure to PCB could result in DNA double-strand breaks.

MCF10A cells treated with PCB153 (1 – 5 μM) resulted in a significant decrease in cell number and an increase in percent non-viable cells at the end of 3-day exposures (Figure 1). Exposure to 4-Cl-BQ (0.5 or 1 μM) did not show any immediate effects on cell number and viability at the end of 3 days. However, 4-Cl-BQ (3 μM) did show an approximately 30% decrease in cell number, but no significant change in the MTS assay. These results suggest 4-Cl-BQ-induced cellular effects might not manifest early while exposure to PCB153 could have immediate cellular effects. Both PCBs reduced the clonogenic properties of cells; 4-Cl-BQ exhibited the most toxic effects. Interestingly, treatment with PEG-catalase prior to and during the PCB exposures suppressed PCB153-induced cytotoxicity while a similar treatment did not significantly alter 4-Cl-BQ-induced cytotoxicity. These results show 4-Cl-BQ to be more toxic than PCB153.

In summary, our results show that exposure to 4-Cl-BQ or PCB153 levels representative of highly exposed individuals elevates ROS levels in MCF10A human nonmalignant breast epithelial cells, leading to DNA damage and cytotoxicity. These results support our hypothesis that cellular ROS can be a significant factor in PCB-induced cytotoxicity. The application of antioxidants could be a viable redox-based countermeasure for PCB-exposed individuals.

Acknowledgements

We thank Dr. Marlan Hansen for assistance with microscopy; Mr. Burl E. Hess and the Flow Cytometry Facility, Central Microscopy Research Facility, and the staff of the ESR Facility at The University of Iowa. Funding from NIEHS (P42 ES 013661) and NIH (CA 111365) supported this work.

ABBREVIATIONS

4-Cl-BQ, 2-(4-chlorophenyl) benzo-1, 4-quinone; CuZnSOD, copper zinc superoxide dismutase; DMPO, 5,5-dimethyl-1-pyrroline N-oxide; EPR, electron paramagnetic resonance; DMSO, dimethyl sulfoxide; MTS, 3-(4,5-dimethylthiazol-2-yl)-5-(3-carboxymethoxyphenyl)-2-(4-sulfophenyl)-2H-tetrazolium; PCB153, 2,2',4,4',5,5'-hexachlorobiphenyl; ROS, reactive oxygen species.

REFERENCES

1. Safe S. Toxicology, structure-function relationship, and human and environmental health impacts of polychlorinated biphenyls: progress and problems. Environ. Health. Perspect 1993;100:259–268. [PubMed: 8354174]
2. Giesy JP, Kannan K. Dioxin-like and non-dioxin-like toxic effects of polychlorinated biphenyls (PCBs): Implications for risk assessment. Crit. Rev. Tox 1998;28:511–569.
3. Gustavsson P, Hogstedt C, Rappe C. Short-term mortality and cancer incidence in capacitor manufacturing workers exposed to polychlorinated biphenyls (PCBs). Am. J. Ind. Med 1986;10:341–344. [PubMed: 3098097]
4. Brown DP. Mortality of workers exposed to polychlorinated biphenyls--an update. Arch. Environ. Health 1987;42:333–339. [PubMed: 3125795]
5. Bertazzi PA, Riboldi L, Pesatori A, Radice L, Zocchetti C. Cancer mortality of capacitor manufacturing workers. Am. J. Ind. Med 1987;11:165–176. [PubMed: 3103429]
6. Sinks T, Steele G, Smith AB, Watkins K, Shults RA. Mortality among workers exposed to polychlorinated biphenyls. Am. J. Epidemiol 1992;136:389–398. [PubMed: 1415158]
7. Loomis D, Browning SR, Schenck AP, Gregory E, Savitz DA. Cancer mortality among electric utility workers exposed to polychlorinated biphenyls. Occup. Environ. Med 1997;54:720–728. [PubMed: 9404319]
8. Demers A, Ayotte P, Brisson J, Dodin S, Robert J, Dewailly E. Plasma concentrations of polychlorinated biphenyls and the risk of breast cancer: a congener-specific analysis. Am. J. Epidemiol 2002;155:629–635. [PubMed: 11914190]
9. Moysich KB, Menezes RJ, Baker JA, Falkner KL. Environmental exposure to polychlorinated biphenyls and breast cancer risk. Rev. Environ. Health 2002;17:263–277. [PubMed: 12611469]
10. Laden F, Ishibe N, Hankinson SE, Wolff MS, Gertig DM, Hunter DJ, Kelsey KT. Polychlorinated biphenyls, cytochrome P450 1A1, and breast cancer risk in the Nurses' Health Study. Cancer Epidemiol. Biomarkers Prev 2002;11:1560–1565. [PubMed: 12496044]
11. Ritchie JM, Vial SL, Fuortes LJ, Guo H, Reedy VE, Smith EM. Organochlorines and risk of prostate cancer. J. Occup. Environ. Med 2003;45:692–702. [PubMed: 12855910]
12. Furst P. Dioxins, polychlorinated biphenyls and other organohalogen compounds inhuman milk. Levels, correlations, trends and exposure through breastfeeding. Mol. Nutr. Food Res 2006;50:922–933. [PubMed: 17009213]
13. Bake MA, Linnika Z, Sudmalis P, Kocan A, Jursa S, Pike A, Ruce M. Assessment of the exposure of breast milk to persistent organic pollutants in Latvia. Int. J. Hyg. Environ. Health 2007;210:483–489. [PubMed: 17317310]
14. Tan Y, Song R, Lawrence D, Carpenter DO. Ortho-substituted but not coplanar PCBs rapidly kill cerebellar granule cells. Toxicol. Sci 2004;79:147–156. [PubMed: 15056819]
15. Amaro AR, Oakley GG, Bauer U, Spielmann HP, Robertson LW. Metabolic activation of PCBs to quinones: reactivity toward nitrogen and sulfur nucleophiles and influence of superoxide dismutase. Chem. Res. Toxicol 1996;9:623–629. [PubMed: 8728508]
16. Eum SY, Rha GB, Hennig B, Toborek M. c-Src is the primary signaling mediator of polychlorinated biphenyl-induced interleukin-8 expression in a human microvascular endothelial cell line. Toxicol. Sci 2006;92:311–320. [PubMed: 16611624]
17. Du K, Chu S, Xu X. Stimulation of MCF-7 cell proliferation by low concentrations of Chinese domestic polychlorinated biphenyls. J. Toxicol. Environ. Health A 2000;61:201–207. [PubMed: 11036508]
18. Coteur G, Danis B, Fowler SW, Teyssie JL, Dubois P, Warnau M. Effects of PCBs on reactive oxygen species (ROS) production by the immune cells of Paracentrotus lividus (Echinodermata). Mar. Pollut. Bull 2001;42:667–672. [PubMed: 11525284]
19. Hilscherova K, Blankenship A, Kannan K, Nie M, Williams LL, Coady K, Upham BL, Trosko JE, Giesy JP. Oxidative stress in laboratory-incubated double-crested cormorant eggs collected from the Great Lakes. Arch. Environ. Cont. Toxicol 2003;45:533–546.

20. Srinivasan A, Lehmler HJ, Robertson LW, Ludewig G. Production of DNA strand breaks in vitro and reactive oxygen species in vitro and in HL-60 cells by PCB metabolites. Toxicol. Sci 2001;60:92–102. [PubMed: 11222876]
21. Lin CH, Lin PH. Induction of ROS formation, poly(ADP-ribose) polymerase-1 activation, and cell death by PCB126 and PCB153 in human T47D and MDA-MB-231 breast cancer cells. Chem. Biol. Interact 2006;162:181–194. [PubMed: 16884709]
22. Schilderman PA, Maas LM, Pachen DM, de Kok TM, Kleinjans JC, van Schooten FJ. Induction of DNA adducts by several polychlorinated biphenyls. Environ. Mol. Mutagen 2000;36:79–86. [PubMed: 11013405]
23. Umegaki K, Fenech M. Cytokinesis-block micronucleus assay in WIL2-NS cells: a sensitive system to detect chromosomal damage induced by reactive oxygen species and activated human neutrophils. Mutagenesis 2000;15:261–269. [PubMed: 10792021]
24. Jagetia GC, Venkatesha VA. Effect of mangiferin on radiation-induced micronucleus formation in cultured human peripheral blood lymphocytes. Environ. Mol. Mutagen 2005;46:12–21. [PubMed: 15795888]
25. Laurent C, Voisin P, Pouget JP. DNA damage in cultured skin microvascular endothelial cells exposed to gamma rays and treated by the combination pentoxifylline and alpha-tocopherol. Int. J. Radiat. Biol 2006;82:309–321. [PubMed: 16782648]
26. Bakkenist CJ, Kastan MB. DNA damage activates ATM through intermolecular autophosphorylation and dimer dissociation. Nature 2003;421:499–506. [PubMed: 12556884]
27. Taneja N, Davis M, Choy JS, Beckett MA, Singh R, Kron SJ, Weichselbaum RR. Histone H2AX phosphorylation as a predictor of radiosensitivity and target for radiotherapy. J. Biol. Chem 2004;279:2273–2280. [PubMed: 14561744]
28. Amaro AR, Oakley GG, Bauer U, Spielmann HP, Robertson LW. Metabolic activation of PCBs to quinones: Reactivity toward nitrogen and sulfur nucleophiles and influence of superoxide dismutase. Chem. Res. Toxicol 1996;9:623–629. [PubMed: 8728508]
29. Schramm H, Robertson LW, Oesch F. Differential regulation of hepatic glutathione transferase and glutathione peroxidase activities in the rat. Biochem. Pharmacol 1985;34:3735–3739. [PubMed: 4052112]
30. Hansen LG, DeCaprio AP, Nisbet ICT. PCB congener comparisons reveal exposure histories for residents of Anniston, Alabama, USA. Fresenius Environmental Bulletin 2003;12:181–190.
31. Malich G, Markovic B, Winder C. The sensitivity and specificity of the MTS tetrazolium assay for detecting the in vitro cytotoxicity of 20 chemicals using human cell lines. Toxicol 1997;124:179–192.
32. Kalen AL, Sarsour EH, Venkataraman S, Goswami PC. Mn-superoxide dismutase overexpression enhances G2 accumulation and radioresistance in human oral squamous carcinoma cells. Antioxid. Redox Signal 2006;8:1273–1281. [PubMed: 16910775]
33. Menon SG, Sarsour EH, Kalen AL, Venkataraman S, Hitchler MJ, Domann FE, Oberley LW, Goswami PC. Superoxide signaling mediates N-acetyl-L-cysteine-induced G1 arrest: regulatory role of cyclin D1 and manganese superoxide dismutase. Cancer Res 2007;67:6392–6399. [PubMed: 17616699]
34. Fenech M, Morley AA. Measurement of micronuclei in lymphocytes. Mutat. Res 1985;147:29–36. [PubMed: 3974610]
35. Fenech M, Chang WP, Kirsch-Volders M, Holland N, Bonassi S, Zeiger E. HUMN project: detailed description of the scoring criteria for the cytokinesis-block micronucleus assay using isolated human lymphocyte cultures. Mutat. Res 2003;534:65–75. [PubMed: 12504755]
36. Buettner GR. In the absence of catalytic metals, ascorbate does not autoxidize at pH 7: Ascorbate as a test for catalytic metals. J. Biochem. Biophys. Meth 1988;16:27–40. [PubMed: 3135299]
37. Duling DR. Simulation of multiple isotropic spin-trap EPR spectra. J. Magn. Reson. B 1994;104:105–110. [PubMed: 8049862]
38. Panus PC, Radi R, Chumley PH, Lillard RH, Freeman BA. Detection of H_2O_2 release from vascular endothelial cells. Free Radical Biol. Med 1993;14:217–223. [PubMed: 8425723]
39. Buettner GR. Spin trapping: ESR parameter of spin adducts. Free Radical Biol. Med 1987;3:259–303. [PubMed: 2826304]

40. Song Y, Wagner BA, Lehmler HJ, Buettner GR. Semiquinone Radicals from Oxygenated Polychlorinated Biphenyls: Electron Paramagnetic Resonance Studies. Chem. Res. Tox. 2008(In press)
41. Eyer P. Effects of superoxide dismutase on the autoxidation of 1,4-hydroquinone. Chem Biol Interact 1991;80:159–176. [PubMed: 1934147]
42. Hall DM, Buettner GR, Mathes RD, Gisolfi CV. Hyperthermia stimulates nitric oxide formation: Electron paramagnetic resonance detection of •NO & hibar; hemoglobin in blood. J. Appl. Physiol 1994;77:548–553. [PubMed: 8002499]
43. Guo Q, Corbett JT, Yue G, Fann YC, Qian SY, Tomer KB, Mason RP. Electron spin resonance investigation of semiquinone radicals formed from the reaction of ubiquinone 0 with human oxyhemoglobin. J. Biol. Chem 2002;277:6104–6110. [PubMed: 11748217]
44. Sakai H, Iwata H, Kim EY, Tsydenova O, Miyazaki N, Petrov EA, Batoev VB, Tanabe S. Constitutive Androstane Receptor (CAR) as a Potential Sensing Biomarker of Persistent Organic Pollutants (POPs) in Aquatic Mammal: Molecular Characterization, Expression Level, and Ligand Profiling in Baikal Seal (Pusa sibirica). Tox. Sci 2006;94:57–70.
45. Wassermann M, Wassermann D, Cucos S, Miller HJ. World PCBs Map: Storage and effects in man and his biologic environment in the 1970s. Ann. New York Acad. Sci 1979;320:69–124. [PubMed: 110205]
46. Johnson-Restrepo B, Kannan K, Rapaport DP, Rodan BD. Polybrominated diphenyl ethers and polychlorinated biphenyls in human adipose tissue from New York. Environ. Sci. Tech 2005;39:5177–5182.
47. Burdon RH, Rice-Evans C. Free radicals and the regulation of mammalian cell proliferation. Free Radical Res. Comm 1989;6:345–358.
48. Goswami PC, Sheren J, Albee LD, Parsian A, Sim JE, Ridnour LA, Higashikubo R, Gius D, Hunt CR, Spitz DR. Cell cycle-coupled variation in topoisomerase II alpha mRNA is regulated by the 3'-untranslated region. Possible role of redox-sensitive protein binding in mRNA accumulation. J. Biol. Chem 2000;275:38384–38392. [PubMed: 10986283]
49. Menon SG, Sarsour EH, Spitz DR, Higashikubo R, Sturm M, Zhang H, Goswami PC. Redox regulation of the G1 to S phase transition in the mouse embryo fibroblast cell cycle. Cancer Res 2003;63:2109–2117. [PubMed: 12727827]
50. Menon SG, Coleman MC, Walsh SA, Spitz DR, Goswami PC. Differential susceptibility of nonmalignant human breast epithelial cells and breast cancer cells to thiol antioxidant-induced G(1)-delay. Antioxid. Redox Signal 2005;7:711–718. [PubMed: 15890017]
51. Menon SG, Goswami PC. A redox cycle within the cell cycle: ring in the old with the new. Oncogene 2007;26:1101–1109. [PubMed: 16924237]
52. Sarsour EH, Agarwal M, Pandita TK, Oberley LW, Goswami PC. Manganese superoxide dismutase protects the proliferative capacity of confluent normal human fibroblasts. J Biol Chem 2005;280:18033–18041. [PubMed: 15743756]
53. Sarsour EH, Venkataraman S, Kalen AL, Oberley LW, Goswami PC. Manganese superoxide dismutase activity regulates transitions between quiescent and proliferative growth. Aging Cell 2008;7:405–417. [PubMed: 18331617]

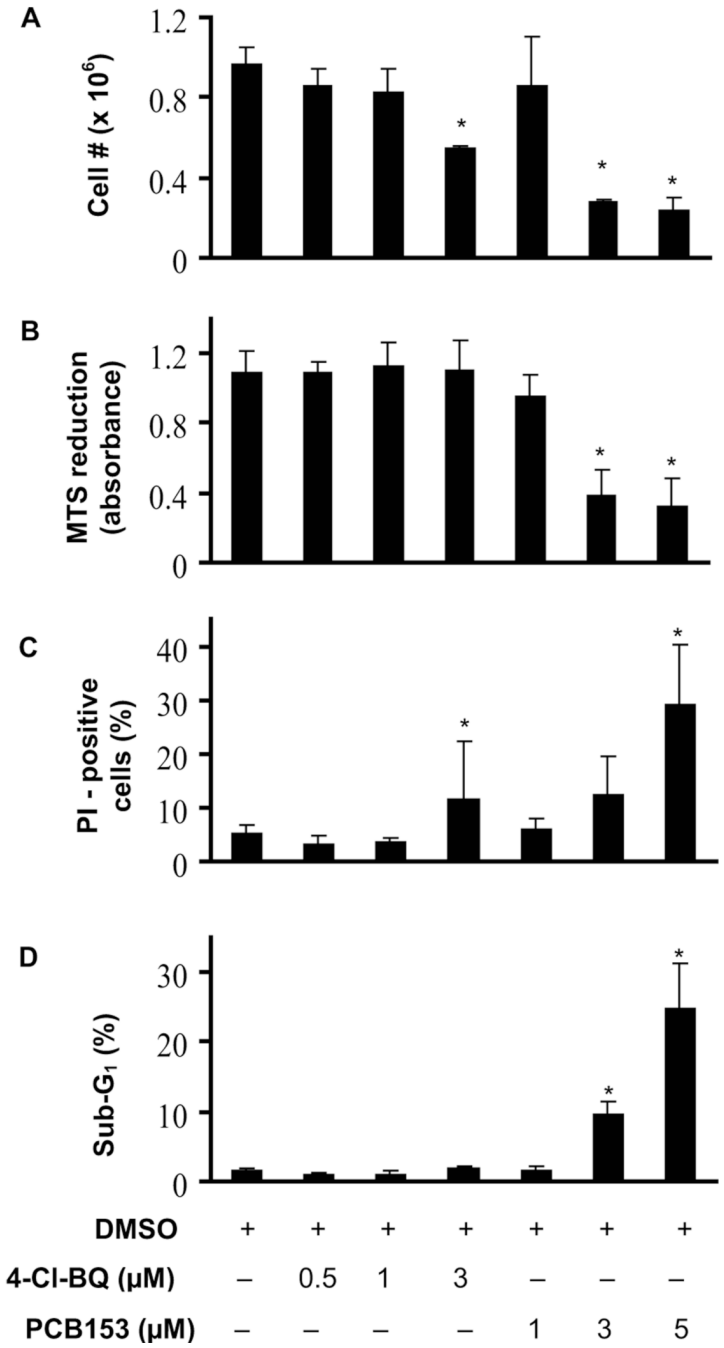

Figure 1. PCB-exposure perturbs cell proliferation

Asynchronously growing exponential cultures of human non-malignant breast epithelial MCF10A cells were exposed to 0–3 μM PCB for 3 days.

(A) Cell number determined for monolayer cultures after trypsinization at the end of 3 days;

(B) Viable cell population was determined *via* the cellular bioreduction of the MTS reagent;

(C) PI-positive (non-viable) and negative (viable) cells were distinguished by flow cytometry. The percentage of PI-positive cells calculated using CellQuest Pro software.

(D) The percentage of cells with sub G_1 DNA content was calculated using ModFit deconvulation software. Cells from replicate dishes were fixed in ethanol and DNA content analyzed by flow cytometry.

(* $P < 0.05$ compared to control)

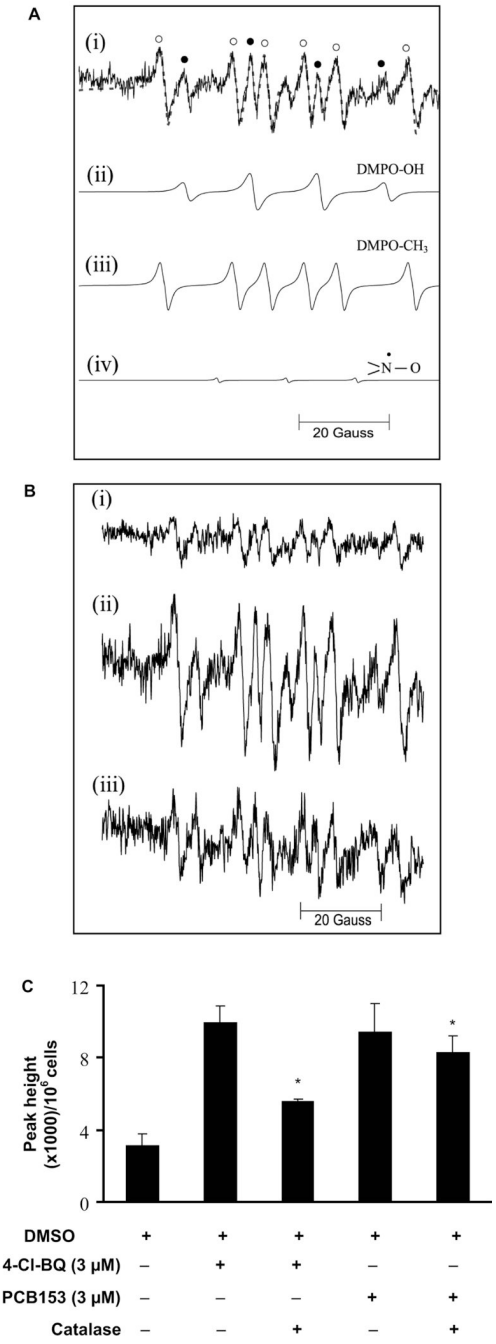

Figure 2. EPR spectroscopy of PCB-induced changes in cellular free radical production

Exponential cultures of MCF10A cells were treated with 3 μM PCB for 3 days followed by incubation with 100 mM DMPO in the presence or absence of 300 U mL^{-1} catalase. **(A)** Experimental and simulated EPR spectra: (i) experimental EPR spectrum of DMPO/PCB-derived radical adducts. The dotted lines represent the simulated spectrum using the NIEHS EPR-simulation program, http://tools.niehs.nih.gov/stdb/esdb.cfm. Spectral hyperfine splittings and species assignments are: (ii) DMPO-OH radical: $a^N = a^H = 14.9$ G; (iii) DMPO-CH_3 radical: $a^N = 15.9$ and $a^H = 23.1$ G, and (iv) nitroxide signal: $a^N = 15.4$ G. The symbols ● and ○ represent spectral lines corresponding to DMPO-OH and DMPO-CH_3 adducts, respectively. The simulated spectrum is a composite of species (ii) – (iv).

(B) Representative EPR spectra of radical adducts from cells treated with DMSO: (i) control; (ii) 3 μM 4-Cl-BQ; and (iii) 3 μM 4-Cl-BQ with catalase. Catalase was added 30 min prior to EPR measurements.

(C) Quantitation of EPR peak heights represents summation of DMPO-OH and DMPO-CH_3 adducts. The peak height of simple nitroxide radical was excluded from the calculation. EPR peak heights were calculated relative to one million cells. (* $P < 0.05$ compared to control; # $P < 0.05$ compared to individual PCB treatments).

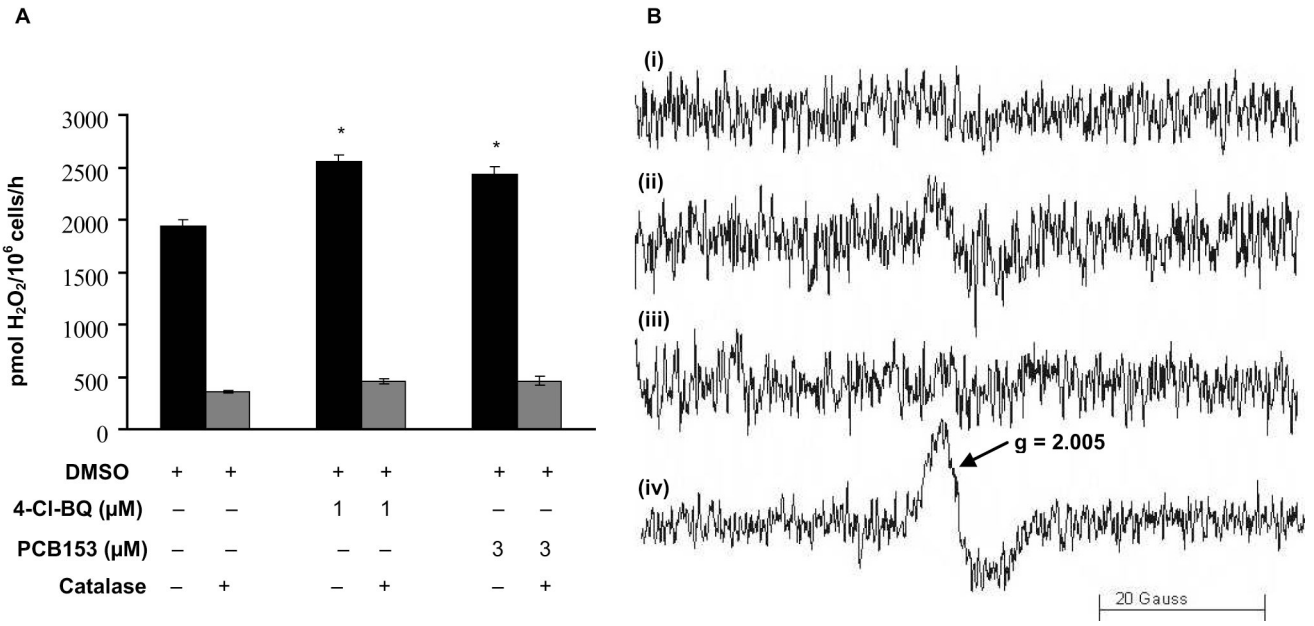

Figure 3. Exposure of MCF10A cells to PCBs increases extracellular H_2O_2 and cell-associated semiquinone radical

(A) H_2O_2 is released from exponentially growing cells treated with PCB for 3 days as measured by spectrofluorimetry. Monolayer cultures were incubated phenol red-free HBSS supplemented with glucose, HEPES, sodium bicarbonate, *p*HPA, and HRP. Catalase (1000 U mL^{-1}) pretreatment was used to determine the specificity of the assay for H_2O_2 measurements. (* $P < 0.05$ compared to control)

(B) A cell-associated immobilized semiquinone radical is observed by EPR in MCF10A cells exposed to 4-Cl-BQ. (i) Control cells (1.5×10^6 cells mL^{-1}), pH 7.4; (ii) cells treated with 4-Cl-BQ, pH 7.4; (iii) Control cells, pH 10; and (iv) cells treated with 4-Cl-BQ, pH 10.

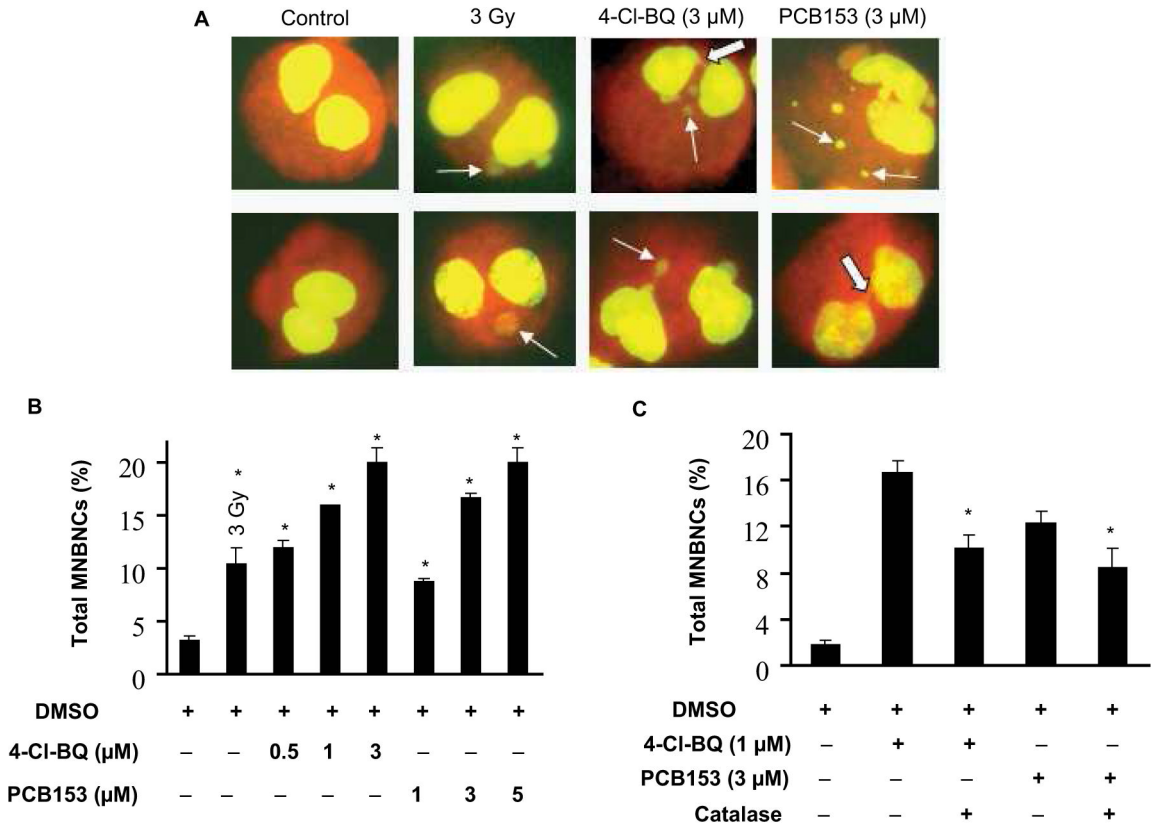

Figure 4. PCB treatment increases DNA damage as seen by micronucleus assay

Monolayer cultures treated with PCBs for 3 days were washed and continued in culture for 2 days in fresh medium containing cytochalasin B. Cells were harvested, fixed, and stained with acridine orange.

(A) Representative microscopic pictures of micronuclei-bearing binucleated cells (MNBNC) in control and PCB-treated cells. Two examples for each treatment are shown. Cells irradiated with 3 Gy were used as positive control for the micronucleus assay. Line-arrows indicate micronucleus (MN) and solid-arrows indicate nucleoplasmic bridge (NPB).

(B) The percentage of cells that contain MNBNC in cultures treated with 0 – 3 μM PCB for 3 days. As a positive control, cells were examined 1 hour after exposure to 3 Gy of ionizing radiation. (* $P < 0.05$ compared to control)

(C) Catalase lowers the frequency of MNBNCs. Exposures to PCB were carried out in absence or presence of 60 U mL^{-1} of PEG-catalase. PEG-catalase was added 1 hour after introduction of PCB, then daily for 3 days.

(* $P < 0.05$ compared to the corresponding PCB-treated groups)

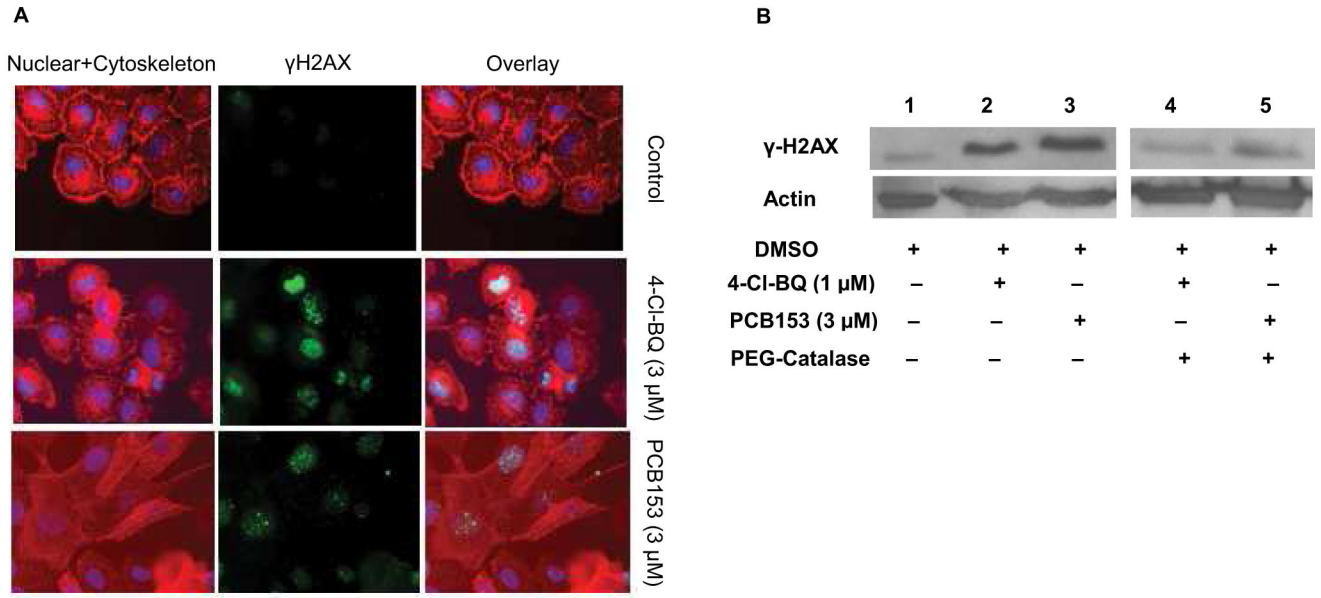

Figure 5. Catalase inhibits PCB-induced increase in phosphorylated histone (H2AX) protein levels

Exponential cultures of MCF10A cells were treated with 3 μM PCB for 3 days and analyzed for γH2AX.

(A) Immunocytochemical staining of γH2AX protein (middle panel, green), nucleus (Hoechst, blue), and cytoskeleton (red); right panel shows overlay images.

(B) Immunoblotting assay of γH2AX protein levels in DMSO-treated control (lane 1) and PCB-treated cells (lanes 2 and 3). Lanes 4 and 5 represent γH2AX protein levels in cells that were treated with PEG-catalase prior to and during the PCB exposures. Actin levels were used for loading correction.

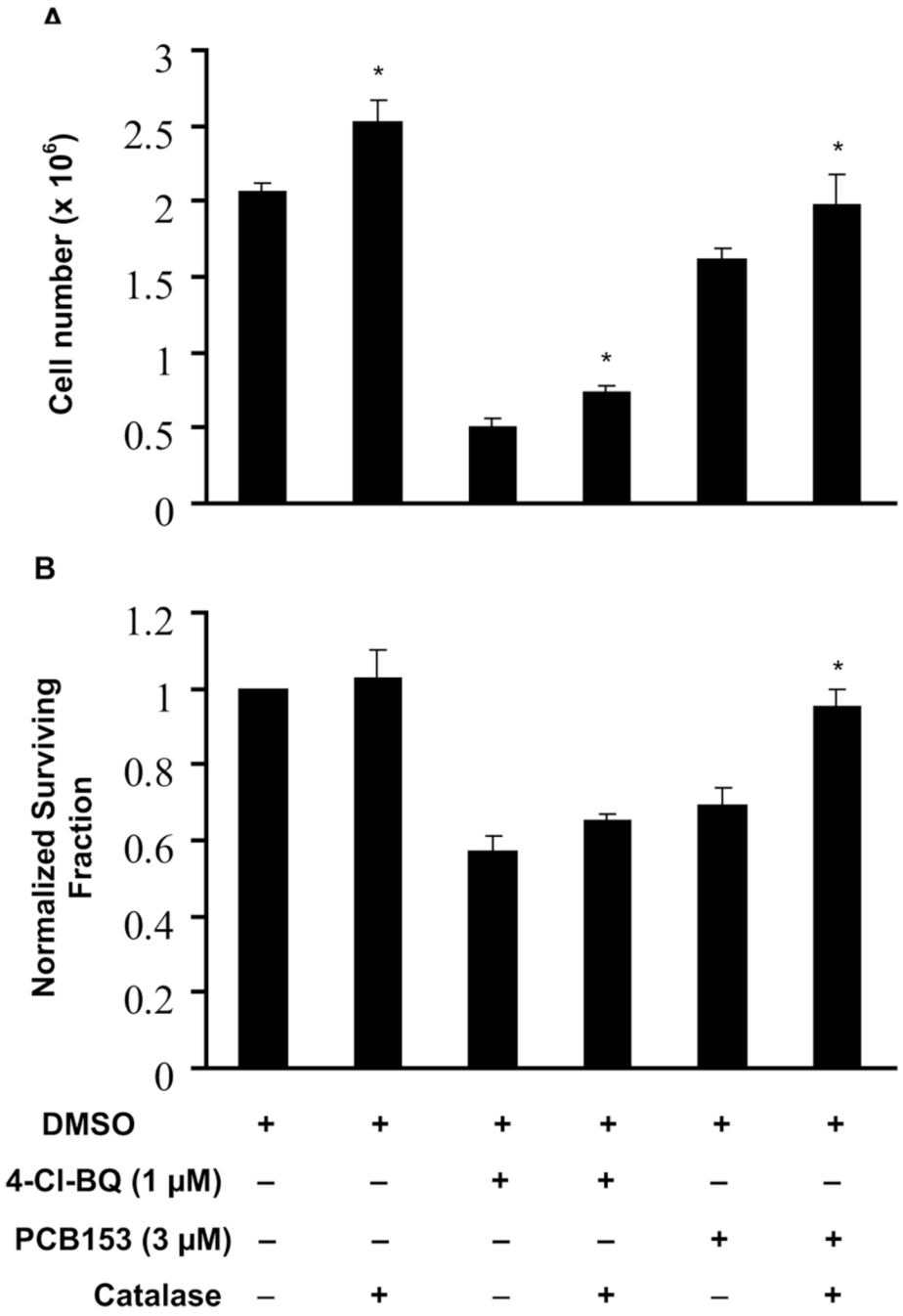

Figure 6. Catalase ameliorates PCB-induced cytotoxicity in MCF10A cells

Monolayer cultures were treated with PEG-catalase prior to and during the 3-day single dose exposure to PCB.

(A) Cell number measurements of monolayer cultures of MCF10A cells. Cells were exposed for 3 days to PCB or vehicle control; cells were harvested and replated in lower numbers in fresh medium with a single dose of PCB or vehicle (+/− PEG-catalase, 60 U mL^{-1}), allowed to grow for 7 days, and then counted.

(B) Clonogenic assay with MCF10A cells exposed to PCB (+/− PEG-catalase). Monolayer cultures were trypsinized at the end of a 3-day PCB-exposure and replated at limiting dilution for clonogenic cell survival assay. At the end of 14 days colonies of cells were fixed and stained.

Each colony with 50 or more cells was counted and surviving fraction was calculated; results were calculated relative to control.
(* $P < 0.05$ compared to the corresponding PCB-treated groups)

Table I

Distributions of micronuclei in 3 d PCB treated MCF10A cells.

Treatment	% MNBNC (mean ± SEM)			NPB	% Total MNBNC (mean ± SEM)
	One MN	Two MN	Multiple MN		
Control	3.2 ± 0.3	0	0	0	3.2 ± 0.3
3 Gy	8.5 ± 1.4	1.5 ± 0.0	0.2 ± 0.5	0.2 ± 0.5	10.5 ± 1.4*
4-Cl-BQ (0.5 μM)	10.2 ± 1.0	1.0 ± 1.0	0.2 ± 0.5	0.5 ± 0.0	12.0 ± 0.7**
4-Cl-BQ (1 μM)	13.5 ± 0.0	1.5 ± 0.0	1.0 ± 0.0	0	16.0 ± 0.0**
4-Cl-BQ (3 μM)	15.0 ± 0.7	2.2 ± 0.5	1.7 ± 0.5	1.0 ± 0.0	20.0 ± 1.4**
PCB153 (1 μM)	6.7 ± 1.0	1.0 ± 1.0	0.2 ± 0.5	0.7 ± 0.5	8.7 ± 0.3**
PCB153 (3 μM)	11.2 ± 1.0	2.7 ± 0.5	1.5 ± 0.0	1.2 ± 0.5	16.7 ± 0.3**
PCB153 (5 μM)	14.5 ± 0.0	2.7 ± 1.5	1.5 ± 0.0	1.2 ± 0.5	20.0 ± 1.4**

MNBNC: micronucleated binucleate cell; MN: micronucleus; NPB: nucleoplasmic bridge; SEM: standard error of mean. One way-ANOVA test was applied to calculate significance differences between treatments

* $p < 0.05$

** $p < 0.01$ compared to control and were calculated using one way-ANOVA test.

Table II

Distributions of micronuclei in 3 d PCB treated MCF10A cells in presence and absence of PEG-catalase.

Treatment	% MNBNC (mean ± SEM)			NPB	% Total MNBNC (mean ± SEM)
	One MN	Two MN	Multiple MN		
Control	1.5 ± 0.5	0.1 ± 0.4	0.33 ± 0.5	0	1.8 ± 0.4
4-Cl-BQ (1 μM)	13.8 ± 1.0	1.5 ± 0.5	1.3 ± 0.5	0	16.6 ± 1.0
4-Cl-BQ (1 μM) + CAT	8.5 ± 1.0	1.0 ± 0.6	0.5 ± 0.5	0.3 ± 0.6	10.1 ± 1.1*
PCB153 (3 μM)	10.1 ± 1.1	0	1.1 ± 0.7	0	12.3 ± 1.0
PCB153 (3 μM) + CAT	7.0 ± 0.6	0.3 ± 0.5	0.6 ± 0.5	0.5 ± 0.5	8.5 ± 1.6*

CAT: PEG-catalase; MNBNC: micronucleated binucleate cell; MN: micronucleus; NPB: nucleoplasmic bridge; SEM: standard error of mean. One way-ANOVA test was applied to calculate significance differences between treatments

* $p < 0.01$ compared to respective PCB-treated control.